Technical Report

Reservoir Characterization Research Laboratory

Carbonate Reservoirs

Rock-Fabric Approach to Reservoir Characterization: Seminole San Andres Unit, Gaines County, Texas

F. Jerry Lucia, Fred P. Wang, and Charles Kerans

Funding for this research was provided by Agip, Amoco, ARCO, British Petroleum, Chevron, Conoco, Exxon, Fina, JNOC, Marathon, Mobil, Phillips, Shell Oil, Texaco, TOTAL, and Unocal.

Bureau of Economic Geology
Noel Tyler, Director
The University of Texas at Austin
Austin, Texas 78713-8924

October 1995

CONTENTS

Figures

Plates (pocket)

INTRODUCTION

Characterization of a carbonate reservoir for fluid flow simulation is a highly complicated task. What is clear is that the end product must be a three-dimensional numerical image of petrophysical properties: porosity, fluid saturation, permeability, and relative permeability. The principal problems are (1) determining petrophysical values to be imaged and (2) distributing petrophysical values in space. Petrophysical properties are determined by measurements on core and outcrop material, by calculations using wireline log data, and by well tests and tracers. Methods of distributing the petrophysical values usually involve a combination of geologic and statistical modeling.

This report emphasizes wireline log calculations and geologic modeling using a rock-fabric approach developed in outcrop studies (Lucia and others, 1992; Senger and others, 1993; Kerans and others, 1994). The approach is to construct a detailed chronostratigraphic framework using sequences of geologic features that are related to water depth and to fill the framework with petrophysical attributes using relationships between rock-fabric and petrophysical properties.

Geologic and petrophysical studies of the San Andres Formation in Lawyer Canyon, Algerita Escarpment, Guadalupe Mountains of New Mexico, suggest that (1) petrophysical properties are near randomly distributed within rock-fabric facies; (2) rock-fabric facies are systematically stacked within high-frequency cycles (HFC's); (3) rock-fabric facies can have significantly different petrophysical properties; (4) vertical changes in properties can be abrupt, whereas lateral changes are gradual; and (5) thin, discontinuous, tight mudstone beds are effective vertical barriers to fluid flow. These findings have been applied to a detailed reservoir characterization study of two sections of the Seminole San Andres Unit operated by Amerada Hess Corporation.

SEMINOLE FIELD AND GEOLOGIC SETTING

The Seminole San Andres Unit (fig. 1), located in Gaines County, Texas, lies on the northern Central Basin Platform immediately south of the San Simon Channel. It covers approximately 23 square miles and contains over 600 wells. The field, discovered in 1936, is a solution-gas reservoir with a small initial gas cap. Original oil in place is estimated to be 1,100 MSTB (Galloway and others, 1983). Waterflooding was initiated in 1970 using alternating rows of 160-acre inverted nine-spot patterns. Infill drilling occurred in 1976, converting the pattern to a mixed 80- and 160-acre inverted nine spot. A second infill program took place during 1984 and 1985 that converted the pattern to an 80-acre inverted nine spot. CO_2 flooding began in 1985.

The reservoir produces from the San Andres Formation of Guadalupian age. Seismic data suggest that Seminole field is one of several isolated platforms built during deposition of the lower San Andres that became linked with the rest of the San Andres platform during progradation of the upper San Andres. Core data reveal that the lower 750 ft of the San Andres contains skeletal grainstone and packstone and an open-marine fauna comparable to that of the uppermost Leonardian retrogradational sequence set of the lower San Andres composite sequence found on the Algerita Escarpment (Kerans and others, 1993, 1994). The highstand systems tract is represented by (1) a lower 300 ft of fusulinid wackestones and packstones, (2) 150 ft of upward-shallowing peloidal shallow subtidal to peritidal cycles, and (3) an upper 350 ft of largely anhydritic peritidal deposits.

GEOLOGIC FRAMEWORK

A detailed reservoir characterization was made of two sections of the Seminole San Andres field (fig. 2). Eleven cores covering the reservoir were described in detail. Through an interactive process of core description and correlation, 12 high-frequency cycles (HFC's) were confidently identified in cores and wireline logs of uncored wells (fig. 3) (Kerans and others, 1993). The

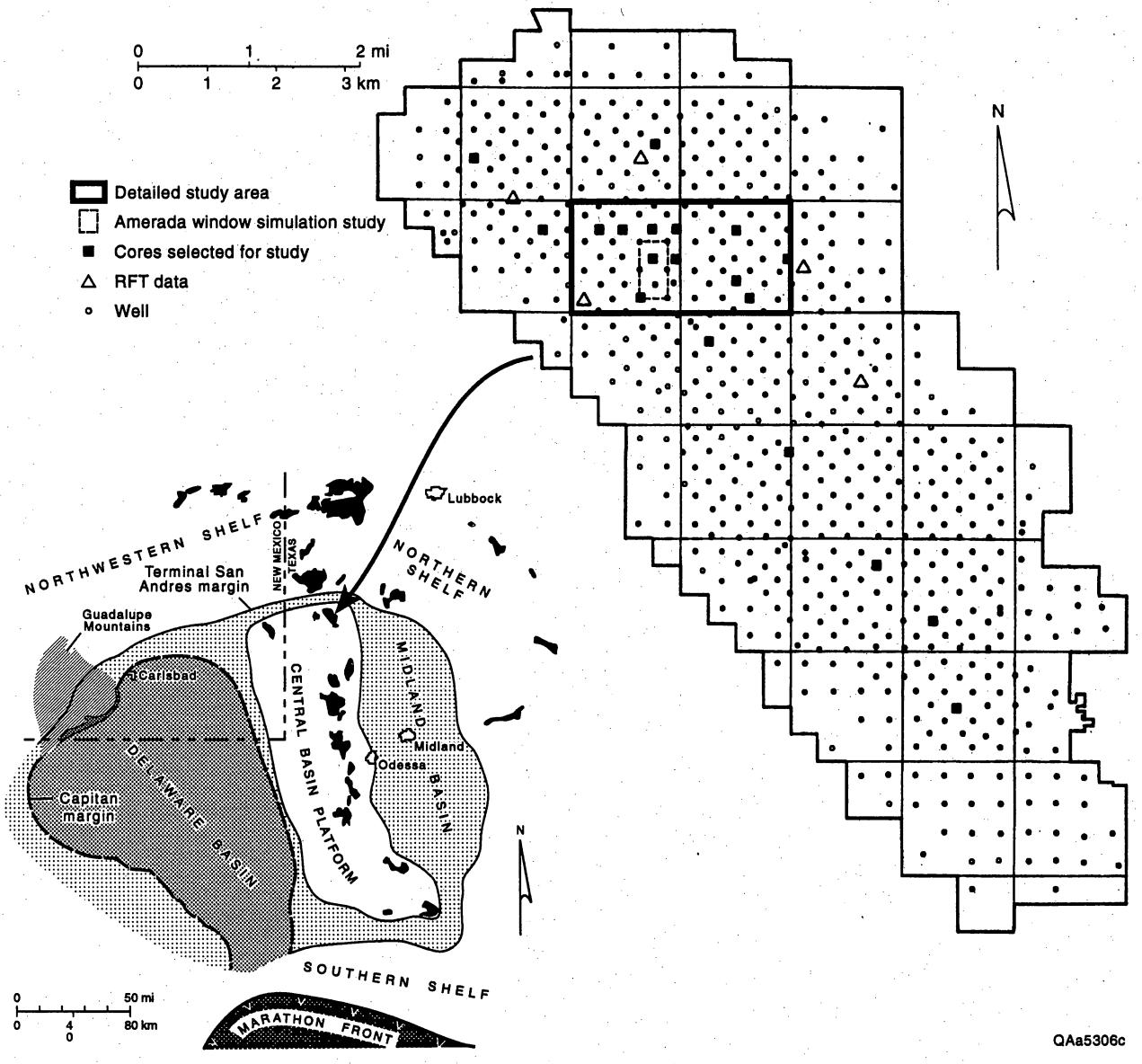

Figure 1. Location map of Seminole field in the Permian Basin, West Texas, and location of the two-section study area (bold outline).

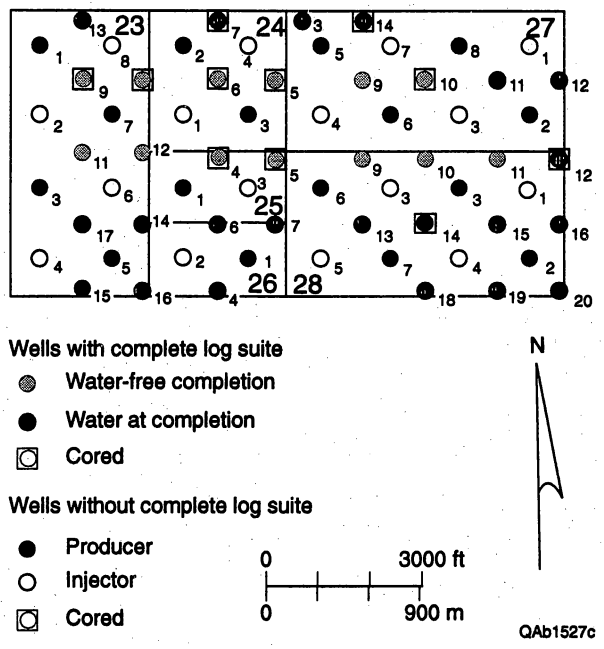

Figure 2. Index map of the two-section study area (base map of tracts 23–28) in the Seminole field, San Andres Unit, Gaines County, Texas.

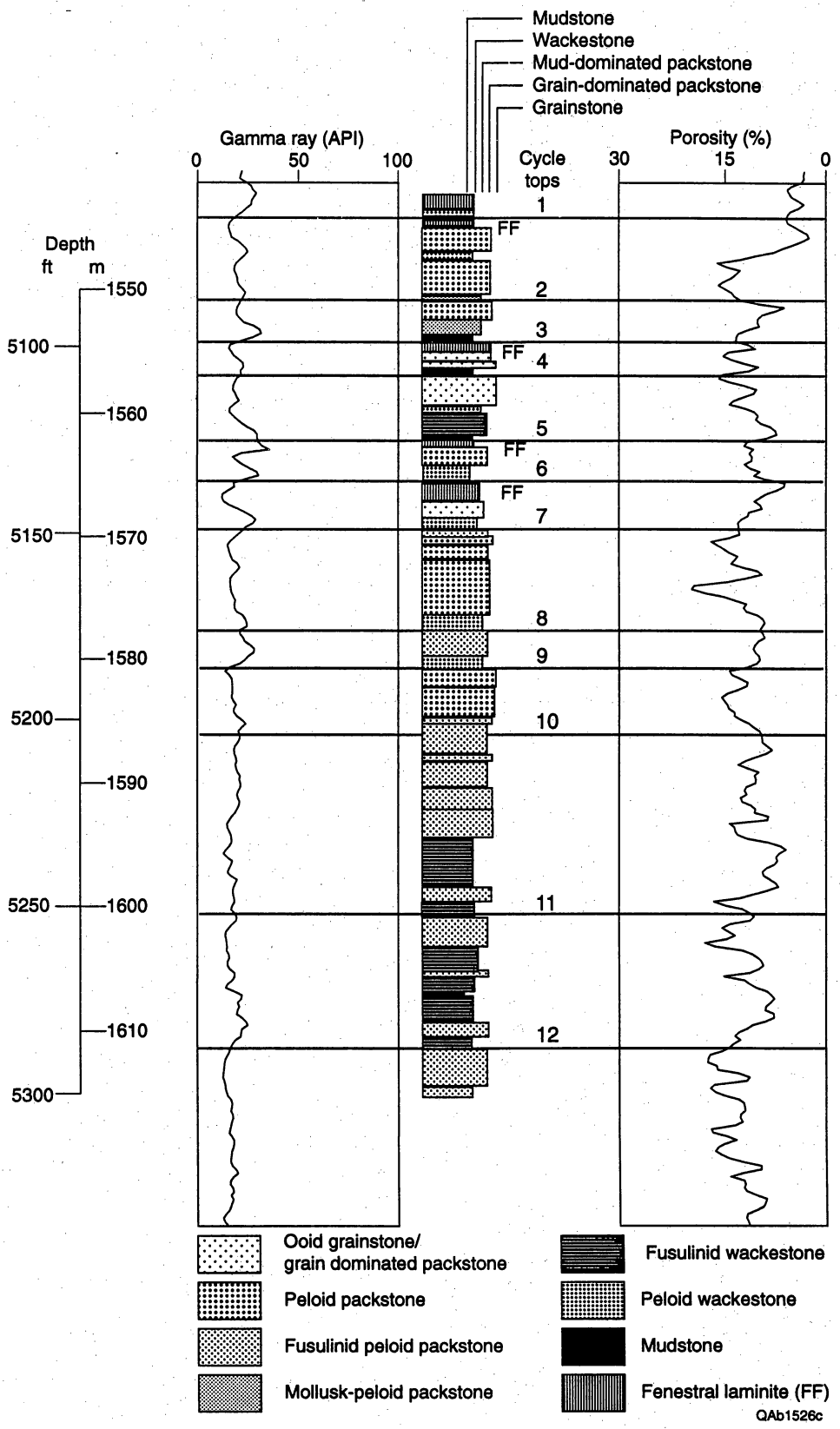

Figure 3. Core description and wireline logs from the Amerada Hess SSAU 2505 well showing high-frequency cycles.

lower three HFC's (cycles 10, 11, and 12) are part of the outer ramp facies tract and are 40- to 50-ft-thick units containing low-porosity, fusulinid-peloid mud-dominated dolostones that coarsen upward into more porous crinoid-fusulinid-peloid grain-dominated dolopackstones.

The upper 9 HFC (cycles 1 through 9) record progradation of the ramp-crest facies tract over the outer ramp. These HFC's are typical upward-shallowing cycles, having basal mudstones and wackestones grading upward into grain-dominated packstones and grainstones (fig. 3). True crossbedded ooid grainstones are rare, but grain-dominated packstones are common. Cycles 2 through 6 shoal locally into fenestral tidal-flat caps, and cycle 1 is overlain by anhydritic peritidal deposits.

QUANTIFICATION OF GEOLOGIC FRAMEWORK

The geologic HFC framework was filled with petrophysical attributes by using rock-fabric data as a basis for integrating core descriptions with core analysis and wireline log data. Data provided by Amerada Hess in the two-section study area included (1) whole-core porosity and permeability data from 11 cores, (2) a limited number of capillary pressure curves and special core analyses, and (3) wireline logs for 58 wells. The logging suite for 33 of the wells drilled between 1970 and 1985 included compensated neutron, density, acoustic, dual laterolog, and microfocused logs. This suite of logs was use in this study.

Core Data

Thin sections were prepared and described from every foot of core from well SSAU 2505. In addition, scattered thin sections were prepared from wells SSAU 2309, 2504, and 2814. Petrophysical rock fabrics were described using the form shown in figure 4, which is based on the Lucia classification (Lucia, 1995). The attributes listed on the form are considered to be the basic elements needed to relate rock fabrics to petrophysics. These are lithology, present-day texture, interparticle porosity, particle size and sorting (grains and/or dolomite crystals), and

DESCRIPTION _____ BY_____DATE_____

Strata	Depth				LITHOLOGY							TEXTURE		PORE TYPE			CORE ANALYSIS	
	Sp. No.	Dolomite		Calc	Sulfate				Quartz		Acc.	Grain Mud	IPPor	P. Size	Vugs (%)		Por	Perm
		%	size	%	Anhy	Type	Gyp	Type	%	Size		0 1	%	um	Svug	Type	%	md

COMMENTS _____

Figure 4. Basic petrographic description form for rock-fabric/petrophysical calibration in nontouching vug reservoirs.

separate-vug porosity and type. The Seminole reservoir does not contain touching vug pore types; therefore, touching vugs were not included as a category on the description form. Porosity and permeability values from core analysis complete the data necessary for rock-fabric–petrophysical analysis.

The porosity–permeability–rock fabric cross plot for well 2505 does not agree with the generic cross plot presented by Lucia (1995), and total porosity measured in thin section is commonly much higher than core porosity, suggesting that the core porosity values are in error (Kerans and others, 1993). To test this possibility, 3 core plugs were drilled from each of 12 whole-core samples from cycles 4 through 8. Although the whole-core samples had been cleaned of hydrocarbons before they were initially analyzed, the plugs were cleaned again. Porosity and permeability were measured on the core plugs before and after the recleaning. The results show that the porosity of the recleaned plugs is several porosity units (PU) higher than that of the plugs before recleaning and that the porosity of the recleaned plugs was on average 2 PU higher than the whole-core porosity (fig. 5a). This suggests that the core was improperly cleaned before whole-core analysis was done, resulting in low porosity measurements. Whole-core permeability falls within the range of the core plug values (fig. 5b), probably because permeability is controlled by large pores and the unremoved hydrocarbons probably reside in very small pores. As will be shown later, the porosity–permeability–rock fabric cross plot using data from the cleaned plugs is consistent with the generic cross plot.

Rock Fabric–Petrophysics Relationships

Petrophysical properties of porosity, permeability, and saturation are a function of pore size distribution, which is related directly to the fabric of the rock. The Seminole San Andres reservoir produces from anhydritic dolomite and contains five principal rock fabrics: (1) dolograinstone; (2) fine to medium crystalline dolomitized grain-dominated packstone; (3) fine crystalline dolomitized mud-dominated packstone, wackestone, and mudstone; (4) medium crystalline mud-dominated dolostone; and (5) separate-vug (moldic) dolostones

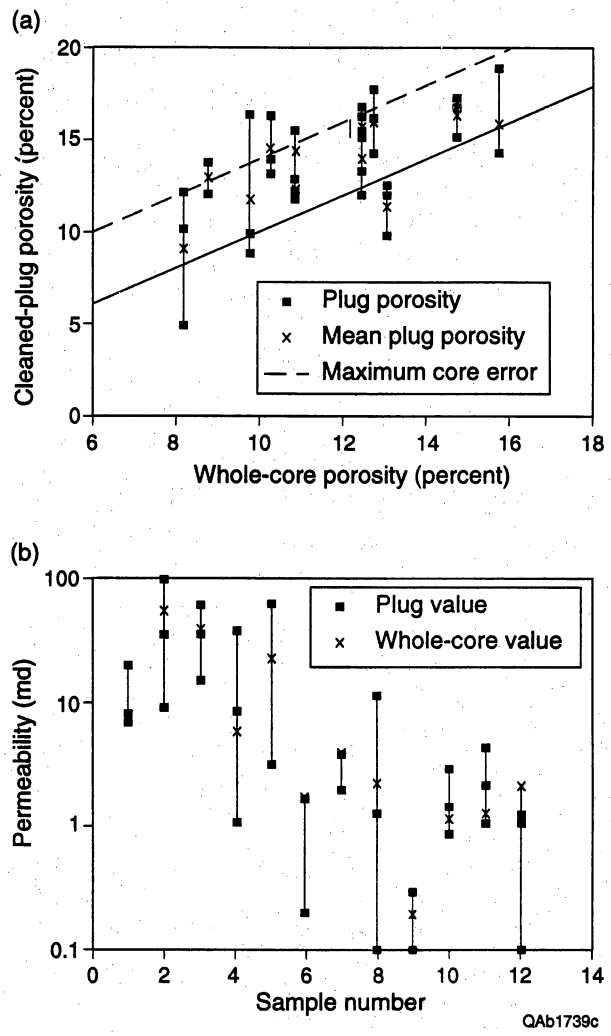

Figure 5. (a) Cross plot of whole-core porosity values versus porosity values of plug samples taken from the whole-core samples and recleaned. Whole-core porosity is too low by 0 to 4 porosity percent. (b) Graphic display showing the range of permeability in selected whole-core samples. Values from three plugs about 1 inch apart are compared with original whole-core values.

(fig. 6). These fabrics have unique stratigraphic locations and, on the basis of generic relationships, unique petrophysical characteristics (Lucia, 1995).

Dolograinstone is the least common fabric in the two-section study area. In this study, the term grainstone is used in the strict sense—a rock with a grain-supported texture and no intergrain lime mud. Grain types generally are either peloids or fusulinids with rare ooids. The generic porosity–permeability cross plot (fig. 7a) shows that this fabric, referred to as petrophysical class 1, has the highest flow potential. However, it is commonly cemented tight with anhydrite. Generic capillary pressure data show that this fabric is characterized by the lowest water saturation (fig. 7b).

Grain-dominated dolopackstones, common in the Seminole reservoir, are often misidentified as grainstones because they are grain supported and may have little intergrain mud. Peloids are the most common grain type. The generic porosity–permeability cross plot shows this fabric to be in petrophysical class 2, having slightly less flow potential than grainstone. Generic class 2 capillary pressure curves characteristically have higher water saturations than those of class 1 grainstones.

Medium crystalline mud-dominated dolostones are very common in the lower cycles. As illustrated by the generic porosity–permeability cross plot, the larger dolomite crystal size shifts mud-dominated fabrics into petrophysical class 2 from class 3 because the intercrystal pores characteristic of medium-sized dolostones are larger than interparticle pores in fine-sized dolostones.

Fine crystalline mud-dominated dolostones (packstones, wackestones, and mudstones) are common in the upper cycles. Common grain types are peloids, mollusk fragments, and fusulinids. The generic porosity–permeability cross plot places this fabric in petrophysical class 3, which has the lowest flow potential. Generic capillary pressure relationships suggest that this class is characterized by the highest water saturation.

Because the whole-core porosity data are of questionable accuracy, only data from the recleaned 36 core plugs taken from cycles 4, 6, and 8 in well 2505 are available to investigate the

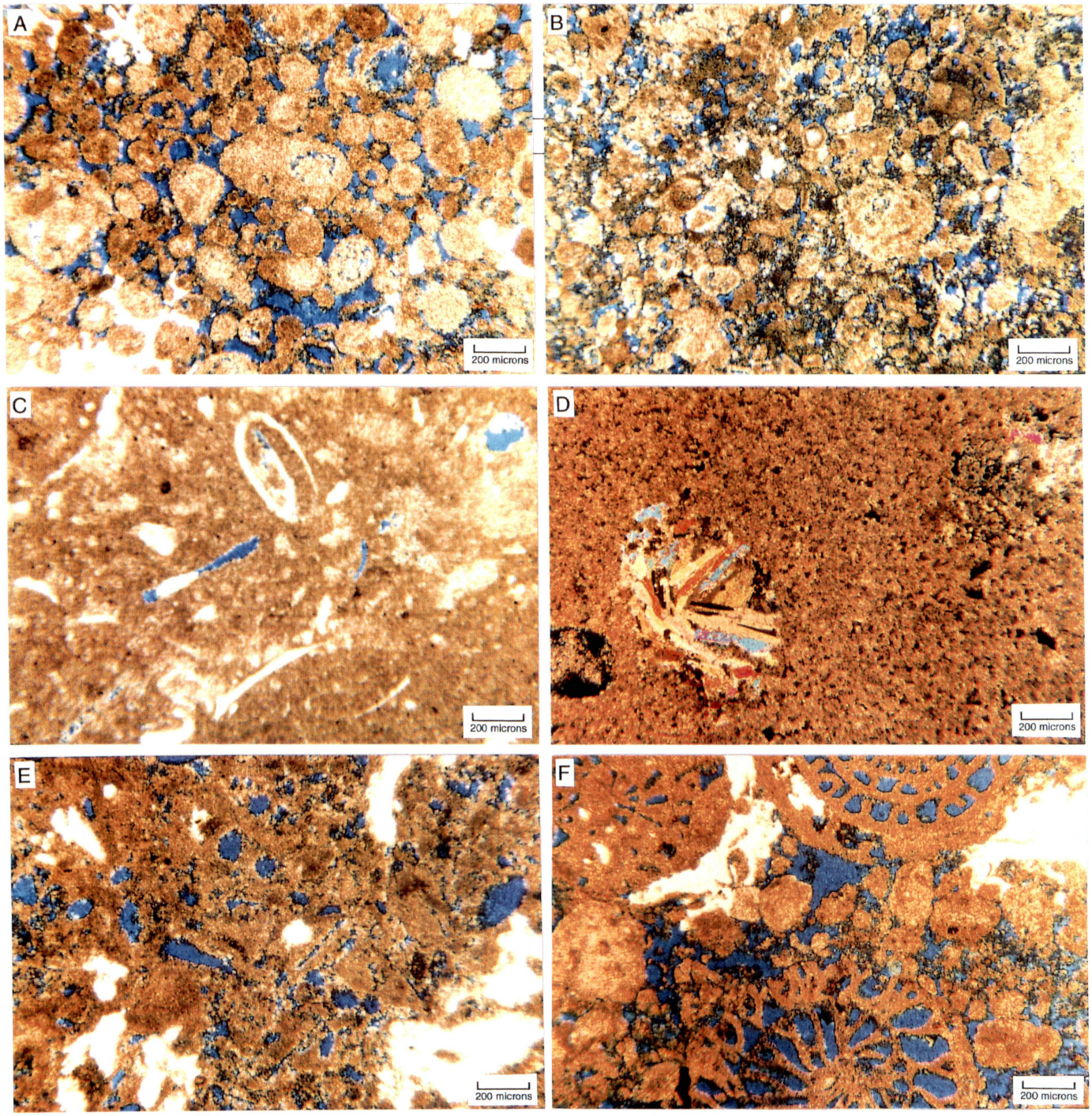

Figure 6. Photomicrographs of thin sections impregnated with blue dye illustrating rock fabrics (white areas are anhydrite): (A) dolograinstone with intergrain pore space, (B) grain-dominated dolopackstone with intergrain pore space and intergrain dolomitized micrite, (C) fine crystalline dolowackestone, (D) medium crystalline dolowackestone (cross polarizers), (E) separate-vug (moldic) porosity in grain-dominated dolopackstone, and (F) separate-vug (intrafusulinid) porosity in grain-dominated dolopackstone.

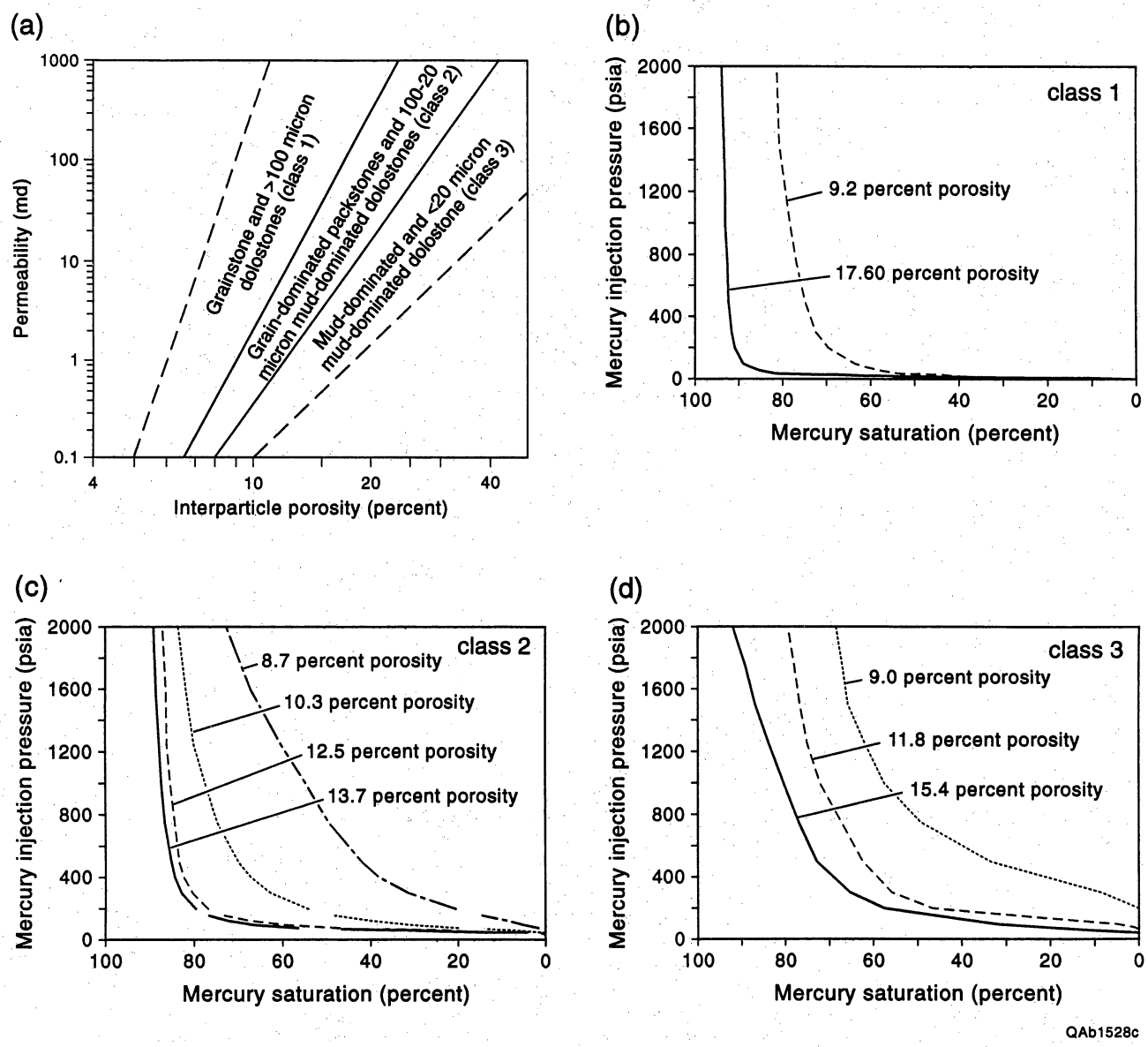

Figure 7. Generic rock fabric, porosity, permeability, and saturation relationships (Lucia, 1995): (a) generic porosity–permeability–rock-fabric relationships and rock-fabric/petrophysical classes cross plot, (b) class 1 generic porosity–saturation–capillary pressure cross plot, (c) class 2 generic porosity–saturation–capillary pressure cross plot and (d) class 3 generic porosity–saturation–capillary pressure cross plot.

relationship between porosity, permeability, saturation, and rock fabric. Unfortunately, none of the samples is from dolograinstones (class 1) or fine crystalline mud-dominated dolostones (class 3). Only grain-dominated dolopackstones and mud-dominated dolostones with 20- to 25-micron dolomite crystals were sampled. In addition, capillary pressure data are insufficient to define saturation–porosity relationships. The porosity–permeability cross plot is shown in figure 8. The grain-dominated fabrics plot well within the class 2 field, whereas the mud-dominated fabrics plot close to the class 2-3 boundary, which is consistent with generic relationships.

Principal separate-vug types are grain molds (dissolved peloids, mollusk fragments, and fusulinids) and intrafusulinid pores. An interval containing separate-vug porosity in the SSAU 2309 well was sampled to investigate the effect of separate vugs on permeability. As is expected from generic relationships, the presence of this pore type reduces permeability over what would be expected if all the pore space was interparticle (fig. 9).

Origin of Vertical Rock Fabric, Petrophysical Properties

The vertical profile of petrophysical properties is a function of the vertical profile of rock fabrics, which are formed by depositional and subsequent diagenetic processes. Depositional textures tend to be systematically stacked vertically within depositional cycles that are related to water depth (fig. 10). The two most common carbonate depositional cycles found on carbonate ramps are (1) upward-coarsening marine cycles and (2) tidal-flat-capped peritidal cycles that coarsen upward in high-energy environments and fine upward in low-energy environments. The simplest diagenetic process is compaction, a physical-chemical process that is a function of pressure and temperature. Diagenetic processes become more complex as various waters flow through the system and react with the rock. Typical waters are marine water driven by compaction and thermal gradients, hypersaline marine water driven by density and hydrodynamic head, meteoric water driven by hydrodynamic head, and burial waters driven by compaction.

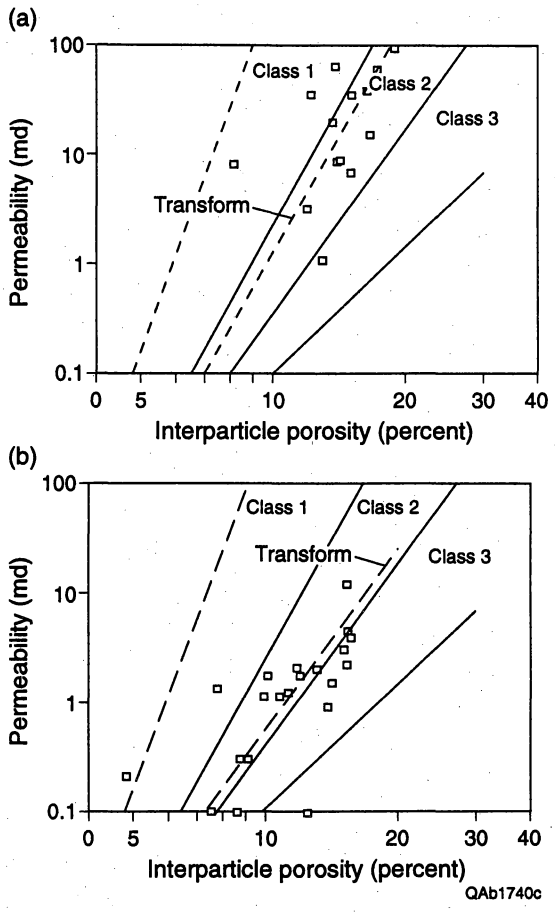

Figure 8. Porosity, permeability, and rock-fabric transforms from core plugs, SSAU 2505 well. (A) Cross plot of interparticle porosity versus permeability for grain-dominated dolopackstone. (B) Cross plot of interparticle porosity versus permeability for dolowackestone with 20-micron dolomite crystals. The three rock-fabric petrophysical classes are shown for comparison.

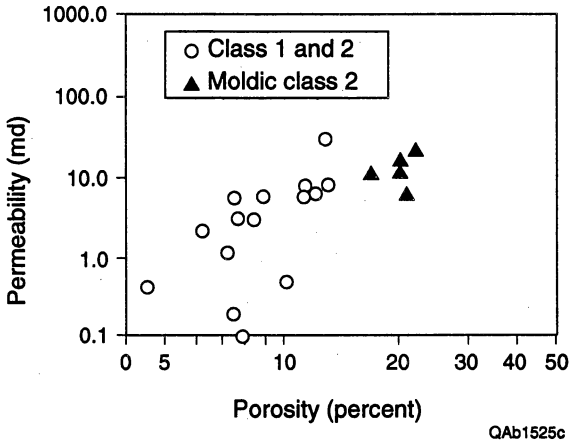

Figure 9. Cross plot of porosity and permeability showing that moldic grain-dominated packstones have lower permeability than expected for grain-dominated packstones with high porosity (SSAU 2309 well).

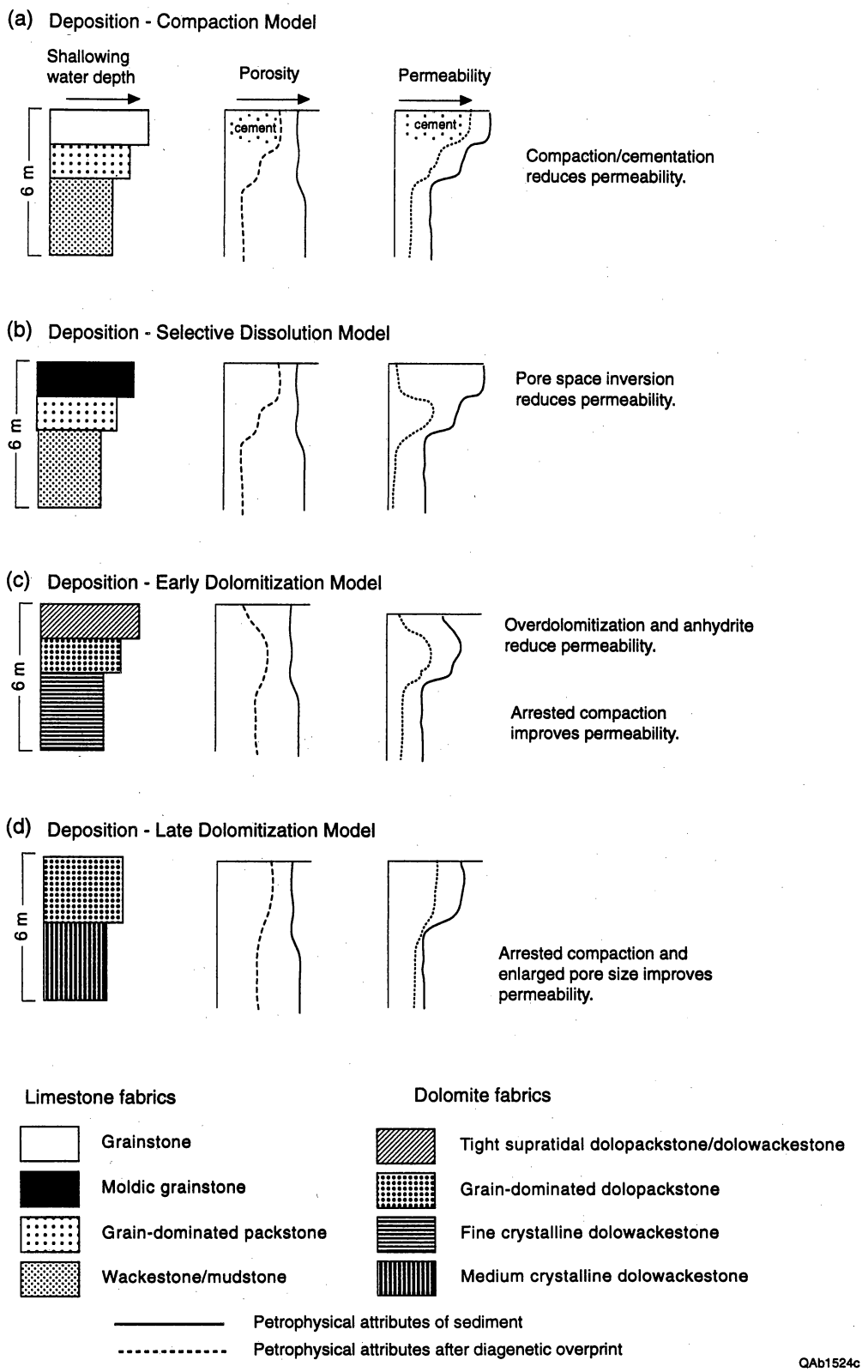

Figure 10. Geologic history of high-frequency cycles present in the Seminole reservoir. (A) Shoaling-upward cycle showing reduction of porosity and permeability resulting from simple compaction/cementation diagenesis. (B) Shoaling-upward cycle showing reduced permeability resulting from selective grain dissolution and associated occlusion of intragrain pore space. (C) Tidal-flat-capped cycle showing early dolomitization, reduction of porosity and permeability caused by overdolomitization and anhydrite precipitation, and improved permeability because of dolomitization arresting compaction. (D) Shallowing-upward cycle showing later dolomitization and improved permeability in dolomitized mud-dominated dolostone caused by increase in particle size and arrested compaction.

The petrophysical characteristics of the depositional–compaction model are controlled by the texture of the depositional cycle and the compactability of the sediment. The compactability of a carbonate sediment is largely related to the ratio of lime mud to grain. Powers (1962) showed how the porosity and permeability of Jurassic limestones decrease with increasing mud to grain ratio. The typical vertical profile that results from the deposition–compaction model is low-porosity mudstone and wackestone grading upward into high porosity grain-dominated sediment (fig. 10). Because permeability is a function of (1) particle size and sorting and (2) interparticle porosity, mudstones and wackestones typically have low porosity and permeability whereas grain-dominated fabrics typically have high porosity and permeability.

The vertical porosity and permeability profiles can be reversed by cementation of the grain-dominated sediments caused by high water flows related to their high permeability. This may result in loss of porosity and permeability in the grain-dominated fabrics but retention of porosity and permeability in the mud-dominated fabrics. Echinoderm grainstones are especially susceptible because of the relative ease of rim cementation growth. In the Seminole field and other San Andres/Grayburg fields, ooid grainstones are commonly cemented with anhydrite or gypsum originating from hypersaline waters associated with dolomitization.

The diagenetic history of tidal-flat cycles is typically more complicated because the tidal flat is periodically exposed, resulting in the introduction of alien waters. The introduction of various waters at the sediment and air surface often results in the loss of porosity and permeability. This is also true of subtidal cycles that are capped by subaerial exposure surfaces.

Hypersaline water is commonly introduced from tidal-flat surfaces and may result in early dolomitization of the depositional cycle (fig. 10). Overdolomitization and anhydrite precipitation in the peritidal sediments may significantly reduce porosity and permeability. Early dolomitization does not necessarily alter the rock fabric when the dolomite crystal size mimics the limestone texture. However, dolomitization can arrest compaction, resulting in porosity and corresponding permeability values that are higher than expected. The upper part of the Seminole

reservoir is characterized by fine crystalline mud-dominated dolostones thought to have been formed relatively soon after deposition.

The permeability profile can be modified from the compaction profile without altering the porosity profile by (1) grain dissolution and associated intergrain precipitation and (2) increase in particle size through dolomitization. The inversion of the pore space from intergrain to intragrain (moldic, for example) results in a significant loss in permeability with little change in porosity (fig. 10). Two cycles in the Seminole field have significant volumes of moldic grainstones that have lower permeability than would be expected for the porosity.

Dolomitization typically produces dolomite crystals ranging in size from a few to hundreds of microns. Assuming no change in porosity, the increase in particle size from lime mud, typically 10 microns, to dolomite with a crystal size of 50 microns increases the permeability by a factor of 10 because of the associated increase in interparticle pore size. Therefore, without changing the porosity profile, the permeability of the mud-dominated portion of the depositional cycle can be significantly increased (fig. 10). This improvement is common in the lower cycles of the Seminole reservoir.

Seminole Cycles

Subtidal, Upward-Coarsening Dolomitized Cycles

The most common depositional cycle in the Seminole field is a mud-dominated unit overlain by a grain-dominated unit. Before dolomitization, compaction-cementation was the dominant diagenetic process and probably resulted in a characteristic vertical profile showing an upward increase in porosity and permeability. In general, this porosity profile is characteristic of cycles 2 and 4 and 7 through 12 (fig. 3). Dolomitization probably resulted in a modest loss of porosity because of overdolomitization (Lucia and Major, 1994), but it arrested compaction.

The dolomite crystal size increases with depth from 10–20 microns to 50–100 microns (fig. 11). Dolomite crystals in grain-dominated fabrics are larger than those in mud-dominated

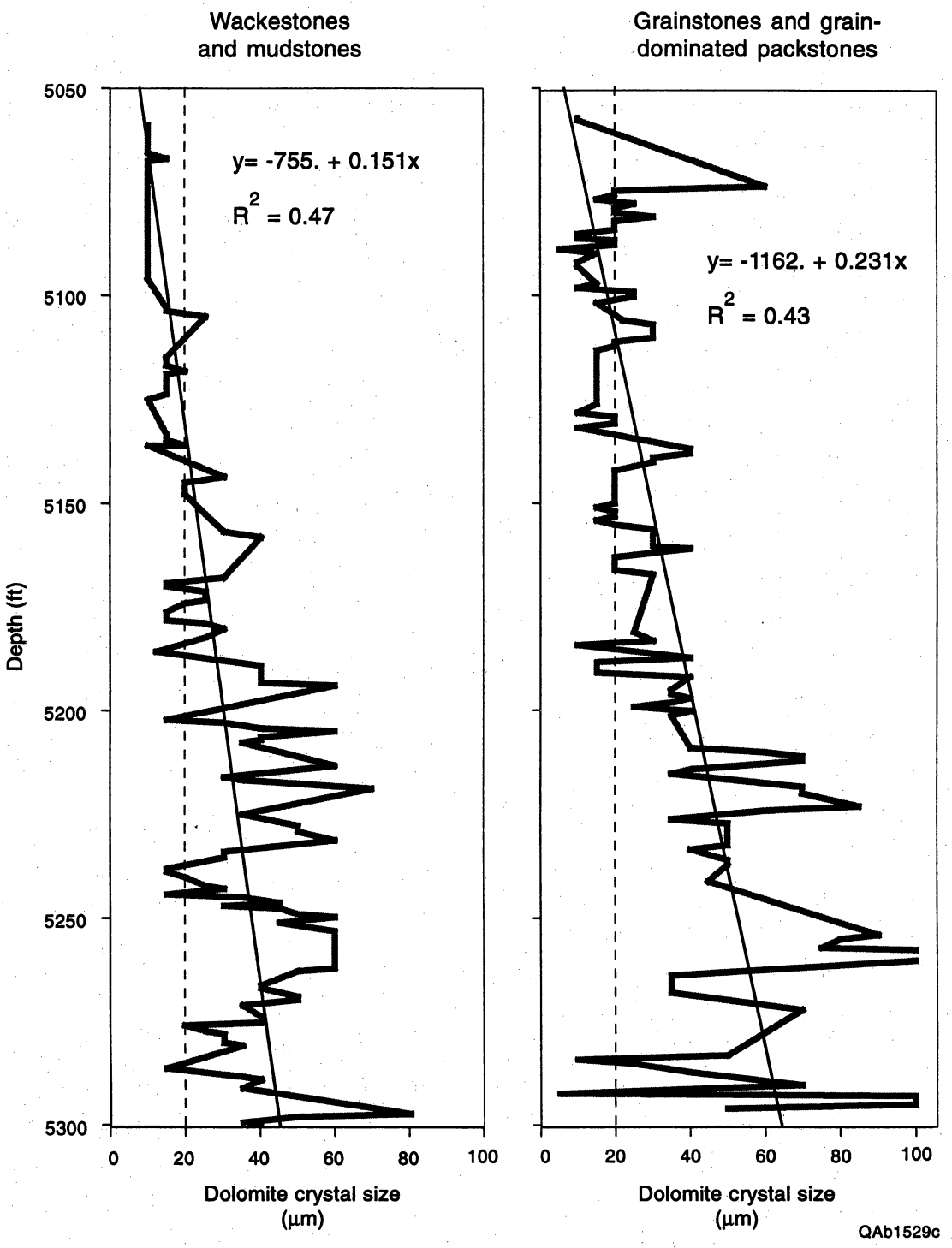

Figure 11. Cross plot of depth versus dolomite crystal size for mud-dominated and grain-dominated dolostones in the SSAU 2505 well showing a somewhat cyclic but systematic increase in crystal size with depth.

fabrics. Mud-dominated fabrics in the upper portion of the reservoir are characterized by fine crystalline dolostones, and the permeability is similar to that expected in limestone. In the lower portion of the reservoir, the dolomite crystal size of mud-dominated dolostone is typically between 20 and 100 microns, and the permeability is higher than that expected in a compacted mud-dominated limestone. Assuming early hypersaline reflux dolomitization from overlying peritidal sediments, the fine crystalline characteristics of the upper portion result from early dolomitization relative to the time of deposition, whereas the medium crystalline characteristics of the lower portion result from later dolomitization relative to the time of deposition.

Tidal-Flat-Capped Dolomitized Cycles

Tidal-flat-capped cycles are concentrated in the dense upper 300 ft of the San Andres Formation. The lithology is a fine crystalline anhydritic dolostone that forms the upper seal for the reservoir and typically has less than 5 percent porosity and 0.1 md permeability. Within the reservoir a few of the upper cycles have discontinuous, thin tidal-flat caps. These tidal-flat caps are also composed of fine crystalline anhydritic fenestral dolostones that are typically tight but rarely have measurable permeability from fenestral pores. The subtidal portion of the cycle is commonly porous and permeable. The result is that porosity in tidal-flat-capped cycles typically decreases upward, as seen in cycles 3, 5, and 6 in figure 3.

Rock-Fabric Flow Units

Outcrop studies suggest that petrophysical properties can be averaged within rock-fabric facies (Lucia and others, 1992). The five rock fabrics described above are the basic building blocks of the Seminole reservoir model, and they have three basic stacking patterns within a cycle:

(1) Fine crystalline mud-dominated dolostone overlain by grain-dominated dolopackstone and dolograinstone.

(2) Fine crystalline mud-dominated dolostone overlain by moldic grain-dominated dolopackstone/dolograinstone. Fusumoldic and intrafusulinid separate vugs are not well organized spatially.

(3) Medium crystalline mud-dominated dolostone overlain by grain-dominated dolopackstone and dolograinstone.

The vertical stacking of the depositional textures as determined by thin-section analysis in well 2505 are compared with the geologic core description in figure 12. In general, the thin-section description is simpler than the geologic description.

Seminole Wireline Log Analysis

Introduction

Only 11 of the 58 wells in the two-section study area have core information. Therefore, methods of extracting accurate values of porosity, saturation, and permeability from wireline log data are needed to increase the density of data before interpolation between wells is attempted. Of the 58 wells, 33 have 3 porosity logs and resistivity logs, the basic logging suite used in this study.

Petrophysical and geological attributes calculated from the wireline logs are total porosity, water saturation, permeability, particle size and sorting, and separate-vug porosity. It is necessary to integrate particle size and sorting information and separate-vug porosity into wireline log calculations because these fabrics control pore size distribution and determine rock-fabric/petrophysical classes.

Porosity

Total porosity is calculated by using TerraStation algorithms and the CNL, density, and acoustic logs. Neutron-density cross-plot porosity is in good agreement with core porosity in well 2505. However, the core porosity has been shown to be too low by several PU. Also, a cross

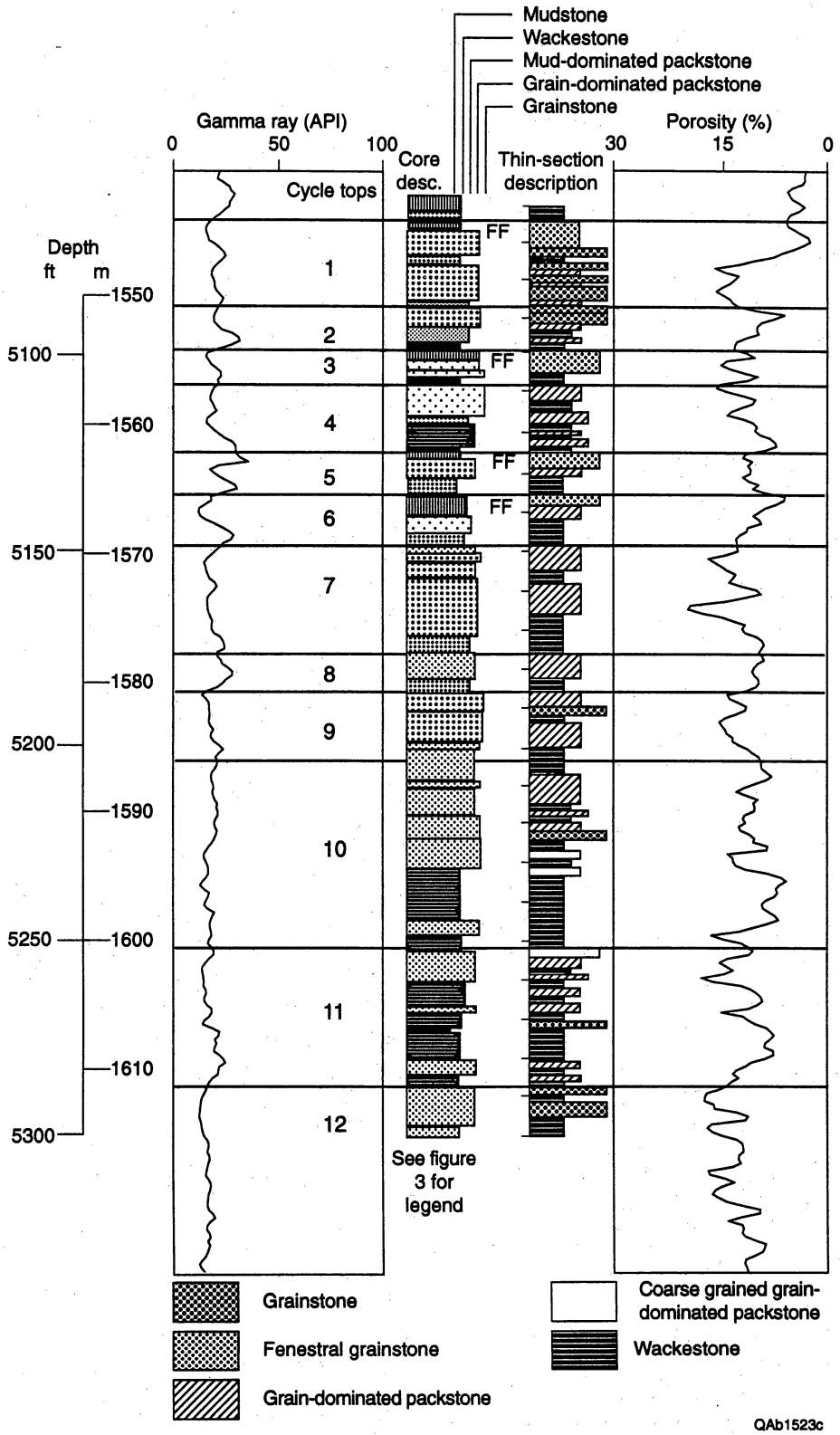

Figure 12. Thin-section description compared with core-slab description and wireline logs from the SSAU 2505 well.

plot of acoustic Δt and neutron-density porosity has an intercept of 48.5 μs/ft, the velocity of limestone, resulting in erroneous grain density values.

The correct lithology was obtained by using the neutron, density, and acoustic logs to calculate porosity using the TerraStation algorithm. A fluid velocity of 150 μs/ft was used because a fluid velocity of 189 μs/ft resulted in significantly low porosity values (Kerans and others, 1993). The porosity values are slightly higher than the core porosity values and agree with the new core analyses. The cross plot of the three-log porosity values and Δt results in an intercept of 46.0 μs/ft, an acceptable value for anhydritic dolomite (anhydrite 50, dolomite 44). The slope of 104 is equivalent to a pseudofluid velocity of 150 μs/ft.

Separate-Vug Porosity

The low Ø/Δt slope is related to the presence of separate-vug porosity (Lucia and Conti, 1987). Lucia and Conti (1987) assumed that the Wyllie time-average equation is correct for carbonate rocks having equal volumes of separate vugs. They developed an empirical equation relating separate-vug porosity to a departure from the ideal, an approach that has been developed by a number of authors (see Wang and Lucia, 1993, for references). Similarly, we have developed an empirical equation relating separate-vug porosity to total porosity and Δt for the Seminole field (see equation below) (fig. 13). The equation is similar to that presented in Lucia and Conti (1987) but has a different intercept because of the difference in velocity of limestone and anhydritic dolomite.

$$\emptyset_{sv} = (2.766 \times 10^{-4}) \times (10^{[-0.1526(\Delta t - 141.5\emptyset)]}) \quad (1)$$

With this equation, total porosity can be divided into interparticle porosity and separate-vug porosity by subtracting total porosity from separate-vug porosity.

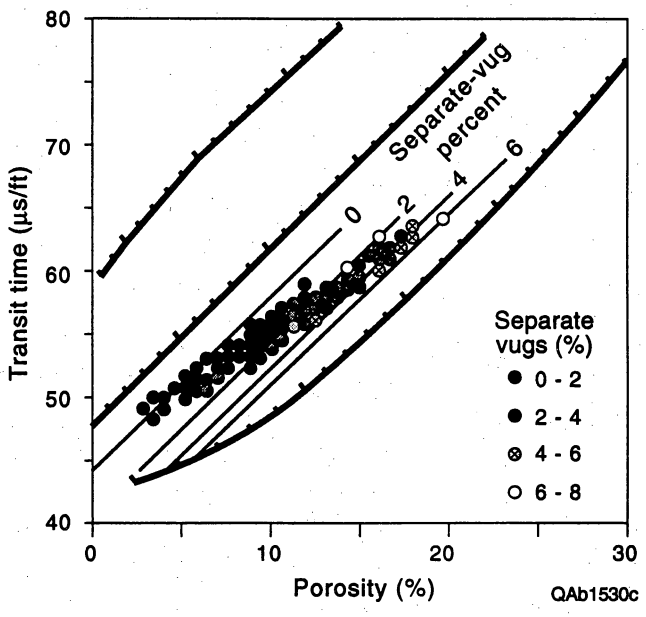

Figure 13. Relationship between transit time, total porosity, and separate-vug porosity in the SSAU 2505 well.

Water Saturation

Water saturations were calculated using the Archie equation and a variable m. A value of 2 was used for the saturation exponent (n), and the resistivity of the original connate water is given as 0.2 ohmm. The cementation factor (m) was calculated from the ratio of separate-vug porosity (calculated from the acoustic–porosity relationship) to total porosity (three-log porosity) using the transform developed with data from Lucia (1983) and Lucia and Conti (1987):

$$m = 2.14(\emptyset_{sv}/\emptyset_t) + 1.76 \quad (2)$$

Particle Size and Sorting

In the absence of touching-vug pore systems, three rock-fabric elements are of primary importance: (1) interparticle porosity, (2) particle size and sorting, and (3) separate-vug porosity. Interparticle porosity is calculated by subtracting log-calculated separate-vug porosity from the total porosity.

Particle size and sorting are estimated by using resistivity curves because resistivity is a function of water saturation, which is a function of pore size distribution, which can be related to particle size and sorting. Particle size and sorting were calculated using a relationship between porosity, saturation, particle size and sorting, and reservoir height. Using data from cycles 1 through 9 in SSAU 2505, water saturations and porosity from log calculations were compared with rock fabrics described from thin sections (fig. 14). A cross plot of average porosity and water saturation shows that fine crystalline mud-dominated dolostones (petrophysical class 3) can be separated from grain-dominated dolopackstones and medium crystalline mud-dominated dolostones (petrophysical class 2). The intervals of grainstone fabrics are too few and too thin for calibration with wireline logs.

The limitations of using water saturation to determine particle size and sorting are listed below.

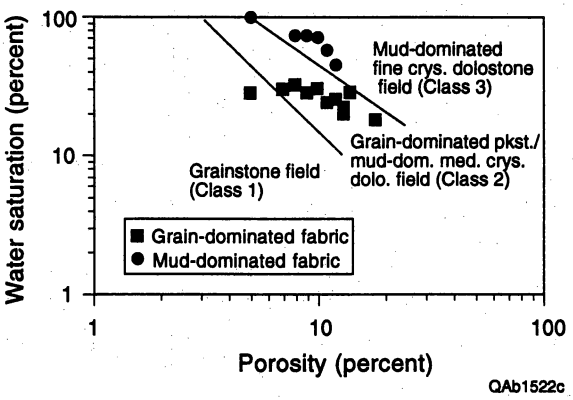

Figure 14. Relationship between water saturation, porosity, and rock-fabric/petrophysical class. The porosity and saturation values have been averaged within rock-fabric units in cycles 1 through 9, SSAU 2505 well.

(1) The method does not work in 100 percent water-saturated intervals. The Seminole logs used to construct the model are all within the oil column.

(2) The height above the zero capillary pressure elevation (herein called reservoir height) must be accounted for. Only intervals well above the zero capillary pressure elevation were used in the Seminole study.

(3) The method will not work in zones that have been waterflooded. In the Seminole field, wells that were completed water free (fig. 2) are considered to have original water-saturation values and original water resistivity. The method was used only in these wells. Wells that were completed producing water and oil are considered to contain water-flooded zones.

Figure 15 shows the point data for three wells and the grouping of fabrics into class 1, 2, and 3. Bounding equations are listed below. Low saturation values have been arbitrarily assigned to class 1. Comparison with core descriptions shows that this group is composed primarily of medium to large crystalline mud-dominated dolostones and contains only a few grainstone fabrics. Therefore, this class 1 is not totally comparable with the generic class 1 of Lucia (1995).

$$\text{Class 1/2 boundary} = Sw = (6.522 \times 10^{-3}) \times (\text{Ø}^{-1.401}) \quad (3)$$

$$\text{Class 2/3 boundary} = Sw = (3.05 \times 10^{-2}) \times (\text{Ø}^{-0.981}) \quad (4)$$

Original water saturations can be estimated using generic relationships between porosity, petrophysical class, and saturation (Lucia, 1995). These estimations compared well with wireline log calculations, and the technique was used to calculate the original water saturations for wells that were completed producing water. For a specific well, the vertical stacking of petrophysical classes was determined by correlation from adjacent wells using the HFC framework as a guide. Saturation values were calculated using petrophysical-class-specific porosity/saturation transforms. The results indicate that flooded zones are restricted to rock-fabric facies, supporting the interpretation that rock-fabric facies are basic elements for reservoir model construction (fig. 16).

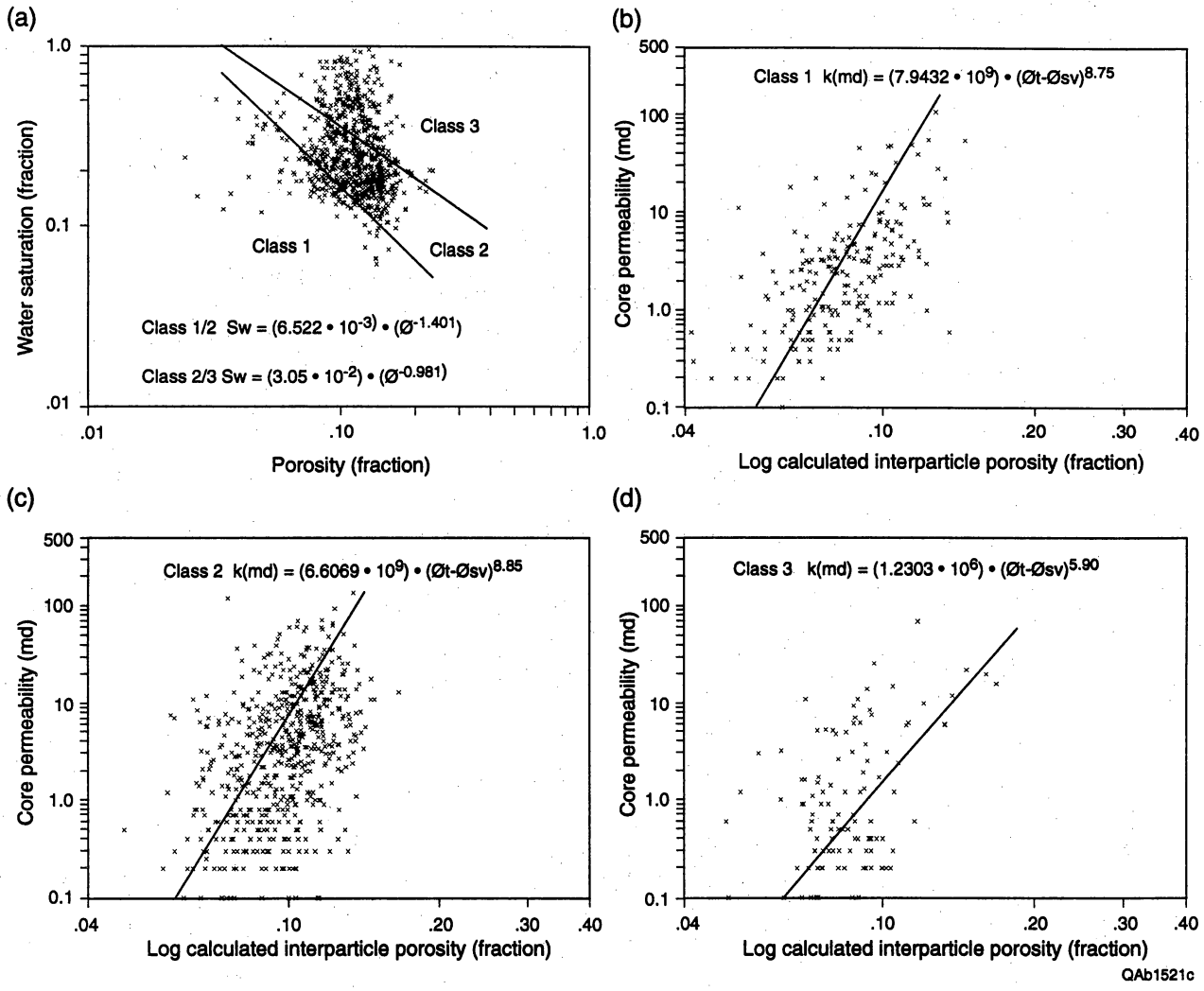

Figure 15. Permeability calculation method. (A) Relationship between water saturation, porosity, and rock-fabric/petrophysical class using point data from well log calculations above transition zone in the SSAU 2505, 2309, and 2504 wells (lines show boundaries between class 1, 2, and 3 used in this study). Cross plots of log-calculated interparticle porosity and core permeability for petrophysical classes identified by the saturation–porosity cross plot and showing the transforms used in this study to calculate permeability: (b) class 1, (c) class 2, and (d) class 3. Notice that the transforms for classes 1 and 2 and not very different.

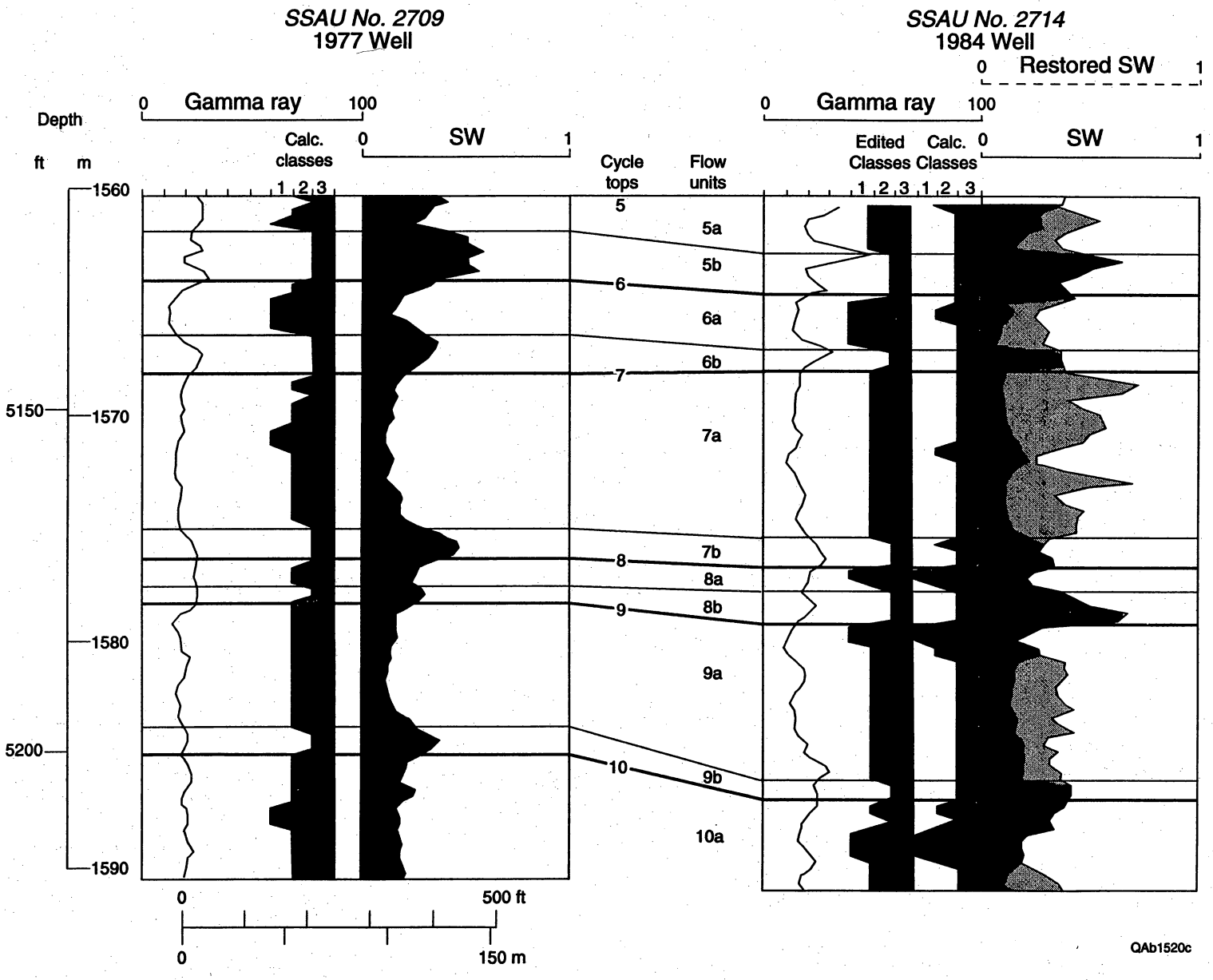

Figure 16. Comparison of log-calculated water saturations in an unflooded well and restored water saturations in a flooded well using porosity and rock-fabric information correlated from adjacent wells and generic equations.

Permeability

Calibrating core permeability with wireline logs is a difficult task. Aside from problems with the accuracy of the core and log data, fundamental problems of calibration include adjusting core depths to log depths and core-analysis depths to core-description depths, averaging core data to equate with wireline log data, and integrating pore size distribution information into the permeability transform. A key consideration, as shown by outcrop and subsurface simulation studies, is that the distribution of high- and low-permeability layers is critical in predicting reservoir performance.

In this study we attempted to use rock fabrics to integrate pore size distribution into the permeability–wireline log transform. The Kozeny equation (Kozeny, 1927) attempts to accommodate pore size distribution by including surface area in the permeability equation. Attributes of the capillary pressure curve and tortuosity factors have also been used (Swanson, 1981). We prefer the rock-fabric approach because it can be related directly to geologic descriptions and therefore allows for accurate quantification of geologic descriptions.

Three rock-fabric/petrophysical classes can be identified by porosity–saturation cross plots (fig. 15). Calibration of these three rock-fabric groups with permeability was done by cross plotting *log-calculated* interparticle porosity and *core* permeability. Averaging the core data and depth-shifting core data to match wireline log data are critical steps. Even when done properly it results in more uncertainty than cross plotting core porosity, permeability, and rock-fabric data measured on the same rock sample. Figure 15 shows cross plots of log-calculated interparticle porosity and core permeability for the three classes from three cored wells. Although there is considerable scatter in the data, the resulting transforms show a shift from class 3, which has the lowest flow potential to class 1, which has the highest flow potential—a trend that is consistent with generic transforms. However, it should be noted that these transforms, especially those of class 3, do not coincide exactly with generic fields based solely on core data. This results from using log-calculated interparticle porosity values rather than core porosity values. Also, class 1

and 2 transforms are very similar, suggesting that class 1 comprises a mixture of class 1 and 2 fabrics, which would be consistent with core descriptions discussed previously.

The permeability transforms used to construct the reservoir model are presented below.

$$\text{Class 1 k(md)} = (7.9432 \times 10^{9}) \times (\text{Øt}-\text{Ø}_{sv})^{8.75} \quad (5)$$

$$\text{Class 2 k(md)} = (6.6069 \times 10^{9}) \times (\text{Øt}-\text{Ø}_{sv})^{8.85} \quad (6)$$

$$\text{Class 3 k(md)} = (1.2303 \times 10^{6}) \times (\text{Øt}-\text{Ø}_{sv})^{5.90} \quad (7)$$

RESERVOIR MODEL CONSTRUCTION

Basic problems in constructing a reservoir model are how to average (upscale) the petrophysical properties defined at the well bore and how to interpolate these properties into the interwell environment. In this study the well bore data are averaged within rock-fabric facies to form rock-fabric flow units. The rock-fabric flow units are correlated between wells within the HFC framework establishing rock-fabric flow layers. The average petrophysical values at each well bore are interpolated between wells within the flow layers, an approach justified because no abrupt lateral changes have been found in outcrop on a similar scale (Lucia and others, 1992).

Outcrop studies (Lucia and others, 1992) describe thin, dense, and discontinuous mud layers that are important barriers to vertical flow. Core descriptions suggest that these dense mud layers are present in the Seminole field as well. However, wireline logs average data over several feet so that the low porosity of these dense layers is averaged with the porosity of adjacent beds. Therefore, the thin, dense, and discontinuous layers had to be inserted into the model based on core descriptions.

Rock-fabric facies from thin-section descriptions, petrophysical classes calculated from porosity and saturation logs, and flow units from the Amerada Hess SSAU 2505 core are shown in figure 17. More detail is shown in plate 1. Calculated rock fabrics in cycles 10 through 12 generally fall into petrophysical class 1 or 2, which is consistent with the core descriptions. The few thin intervals of class 3 are associated with dense dolomudstones. The saturation approach to determining rock fabric becomes unreliable in cycle 12 because of the proximity of the oil-water contact.

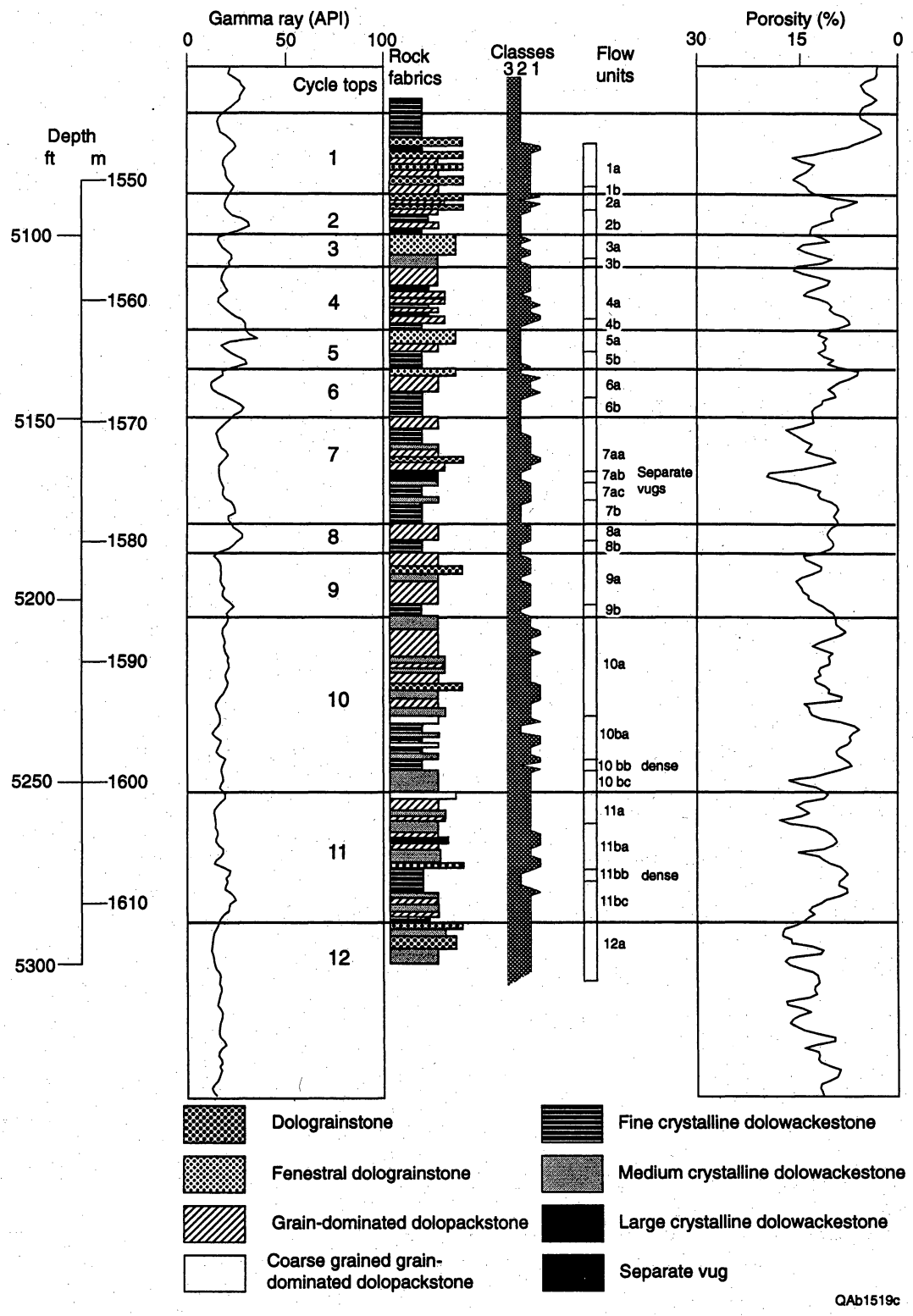

Figure 17. Rock fabrics and permeability calculated from wireline logs and resulting flow unit definition compared with thin-section and core-slab description and with core measurements (SSAU 2505 well).

Because of the uniform rock-fabric/petrophysical characteristics of cycles 10 through 12, log-calculated petrophysical rock fabrics cannot be use to describe flow units. However, core descriptions show that cycles 10 and 11 consist of a lower medium crystalline dolowackestone and an upper medium crystalline grain-dominated dolopackstone and that the packstone has higher porosity than the wackestone, a difference that is probably inherited from differential compaction of the precursor limestone. The porosity difference is also reflected in the permeability. Therefore, definition of flow units in cycles 10 through 12 is based on porosity or permeability because it reflects the depositional texture–compaction model (fig. 10).

Analysis of cycle 11 (fig. 18) illustrates the use of porosity correlated with rock fabric to define rock-fabric flow units. The core description, flow units, gamma-ray log, and a comparison between core-analysis and log-calculated porosity and permeability values are illustrated. Two rock-fabric flow units are defined in cycle 11: a lower low-permeability unit (11b) composed of medium crystalline mud-dominated dolostone, and an upper high-permeability unit (11a) composed of grain-dominated dolopackstone. A laterally persistent dense zone is located within the lower unit (11b) and defines an important barrier to vertical flow. Therefore, cycle 11 is divided into four flow units (in descending order): grain-dominated dolopackstone (11a), medium crystalline mud-dominated dolostone (11ba), dense, fine crystalline mud-dominated dolomudstone (11bb), and medium crystalline mud-dominated dolostone (11bc).

Above cycle 10 the dolomite crystal size tends to mimic the precursor limestone texture, and calculated petrophysical rock-fabric classes 1, 2, and 3 are present. The typical vertical stacking pattern is class 3, overlain by class 2 and rarely class 1. More than 5 percent separate-vug porosity is calculated from the wireline logs in one interval in cycle 7. Because this interval can be traced over a substantial area (fig. 19), it is defined as a separate-vug flow unit (7ab). A second mappable separate-vug flow unit is found in cycle 5 but does not extend into well 2505 (fig. 19).

Analyses of cycles 2 and 3 from well 2505 (fig. 20) exemplify how flow units are defined in the upper cycles. The core description, flow units, gamma-ray log, and a comparison between

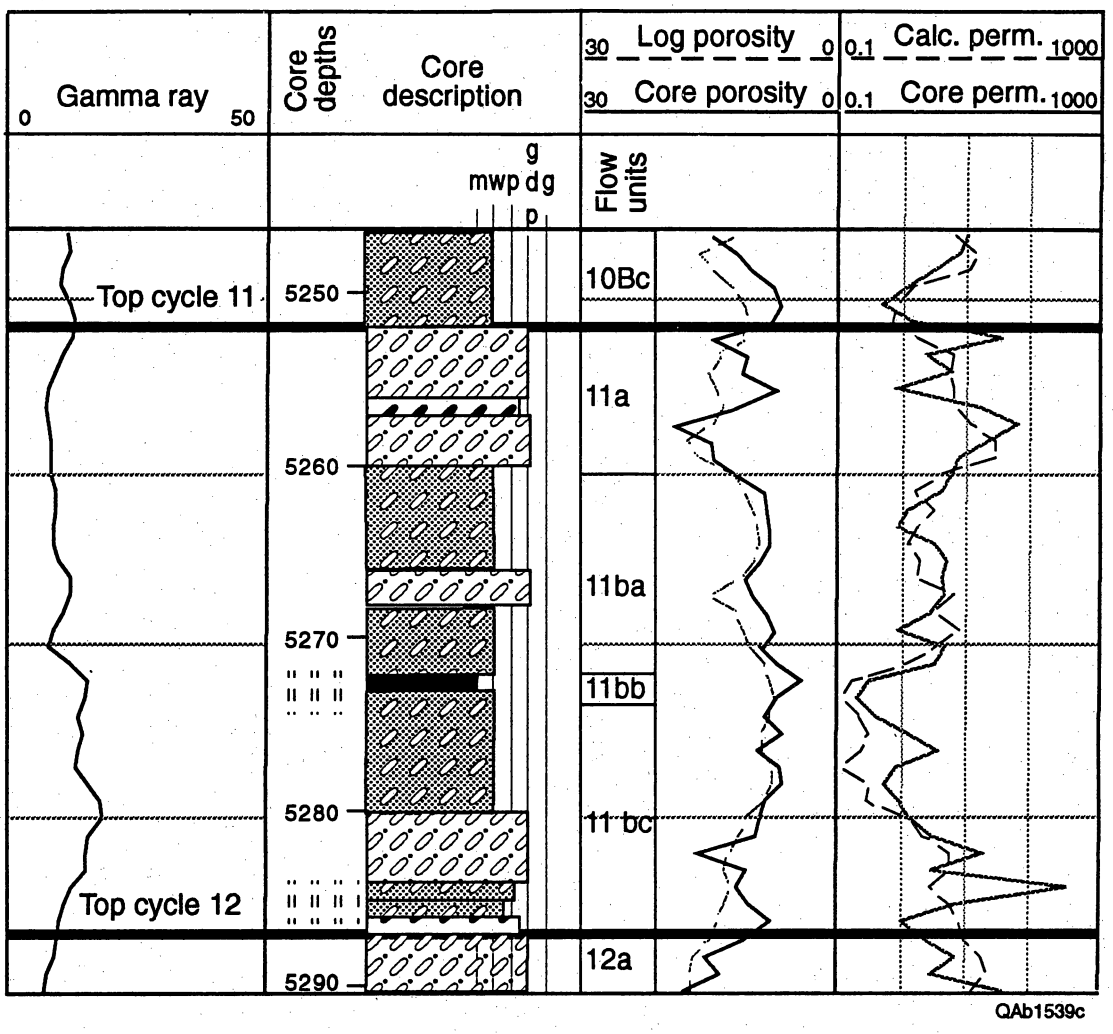

Figure 18. Cycle 11 core description, rock-fabric flow units, core and log-calculated porosity and permeability, and gamma-ray log, SSAU 2505 well.

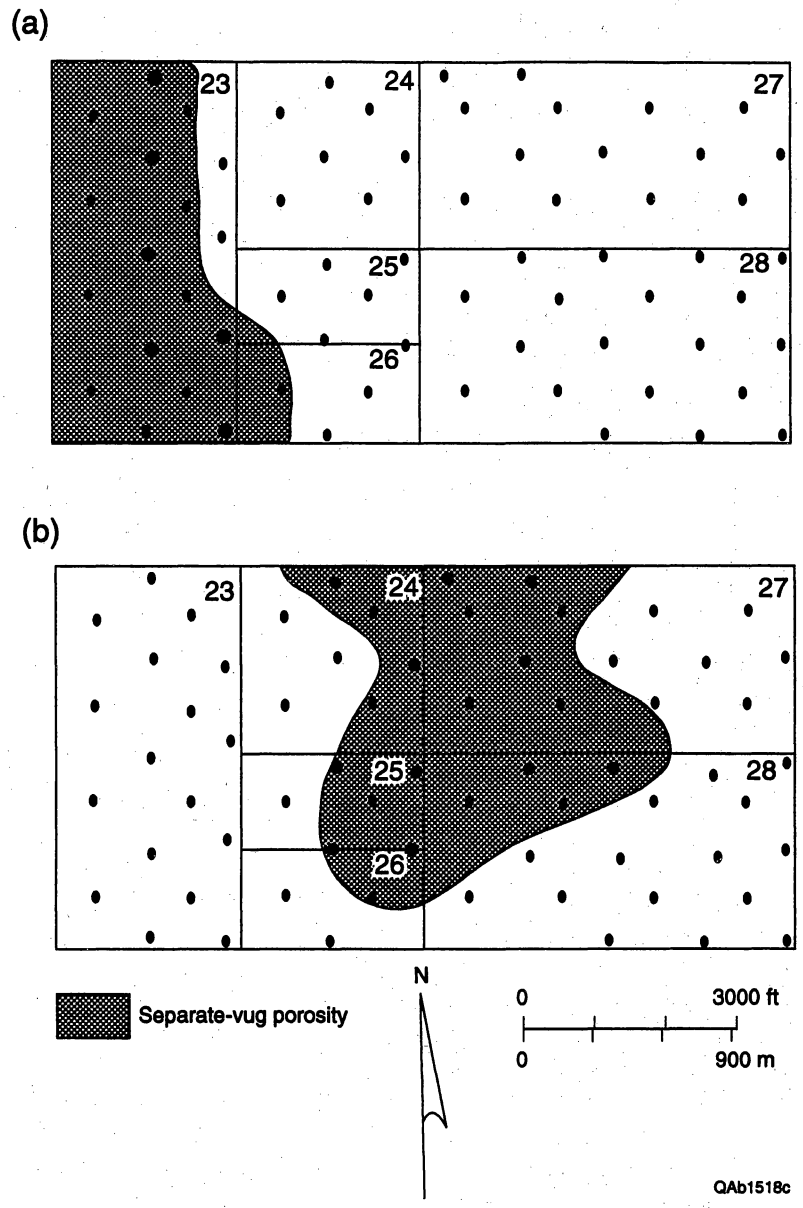

Figure 19. Map of two-section study area showing distribution of separate-vug flow units in (a) cycle 5 and (b) cycle 7. The flow units are between 5 and 10 ft thick.

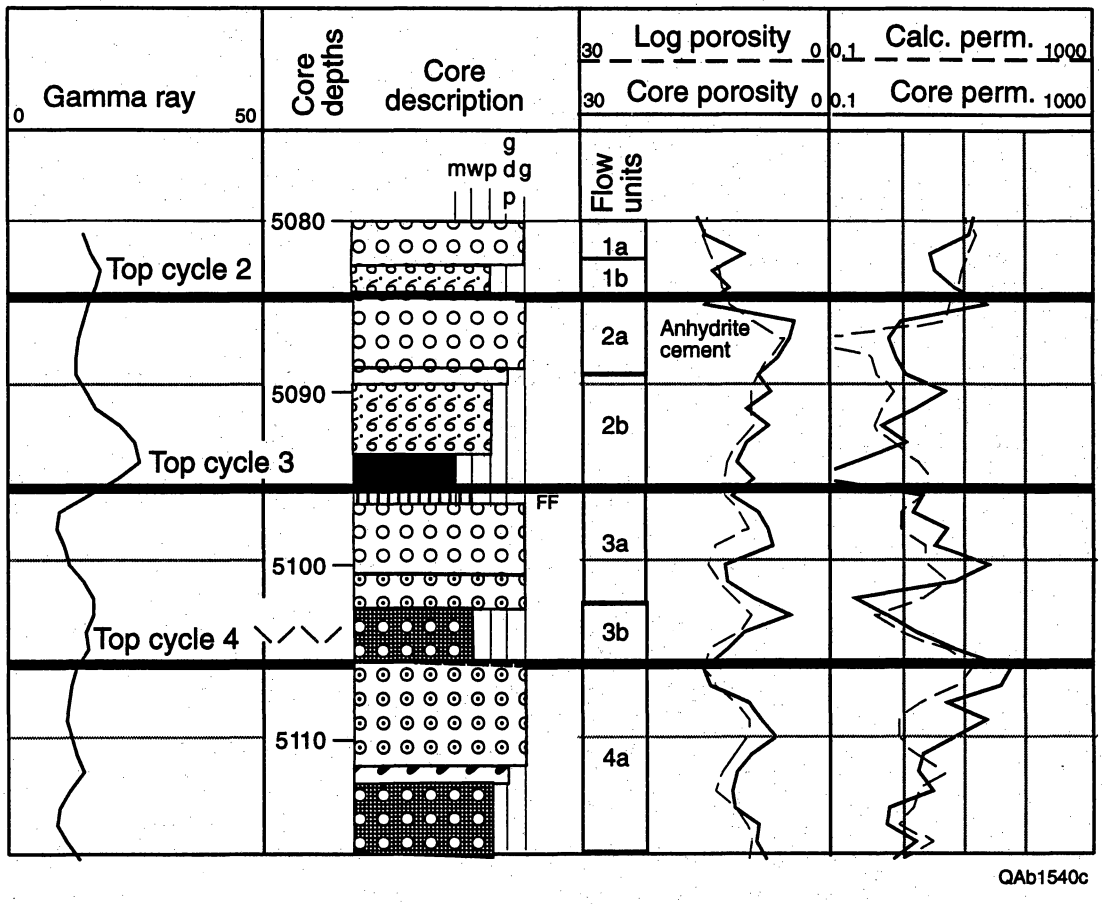

Figure 20. Cycles 2 through 4 core description, rock-fabric flow units, core and log-calculated porosity and permeability, and gamma-ray log, SSAU 2505 well.

core-analysis and log-calculated porosity and permeability values are illustrated. Flow units are defined by the vertical stacking of rock-fabric facies. Cycle 2 has two flow units defined by a lower fine crystalline mud-dominated dolostone (2b) and an upper grain-dominated dolopackstone that is cemented with pore-filling anhydrite (2a). Cycle 3 also has two units defined by fine crystalline mud-dominated dolostone (3b) overlain by a grain-dominated dolopackstone (3a); the cycle has thin fenestral cap.

Rock-fabric flow units are defined in each well and were correlated as constrained by the HFC framework. Because most reservoir simulation programs do not permit discontinuous layers, all flow unit boundaries must be continuous within the model. This results in rock-fabric flow layers containing more than one rock-fabric facies. No sharp boundaries are placed between the facies because no sharp boundaries have been found in analog outcrops on the scale of 1,000 ft, and average petrophysical values are interpolated between wells to fill the HFC framework.

The result is shown in figure 21 and plate 2. The simulation model contains 41 rock-fabric flow layers within the 12 high-frequency cycles. Petrophysical properties vary by several orders of magnitude at a lateral scale of 1,000 ft and a vertical scale of a few feet to tens of feet. This simulation model is considered to be a realistic image of 80 acres in the Seminole reservoir because it is consistent with outcrop studies.

DISCUSSION

The rock-fabric method described herein results in a geologic image that is comparable with outcrop descriptions. It preserves not only the cycle-based geologic framework but also the architecture of petrophysically based rock-fabric facies. The problem of scale averaging is minimized by averaging petrophysical data within rock-fabric facies and using rock-fabric layers for constructing the simulation model. The use of rock-fabric-specific permeability transforms preserves high and low values better than the commonly used single transform, and calculation of separate-vug porosity eliminates overestimation of permeability in zones of high separate-vug

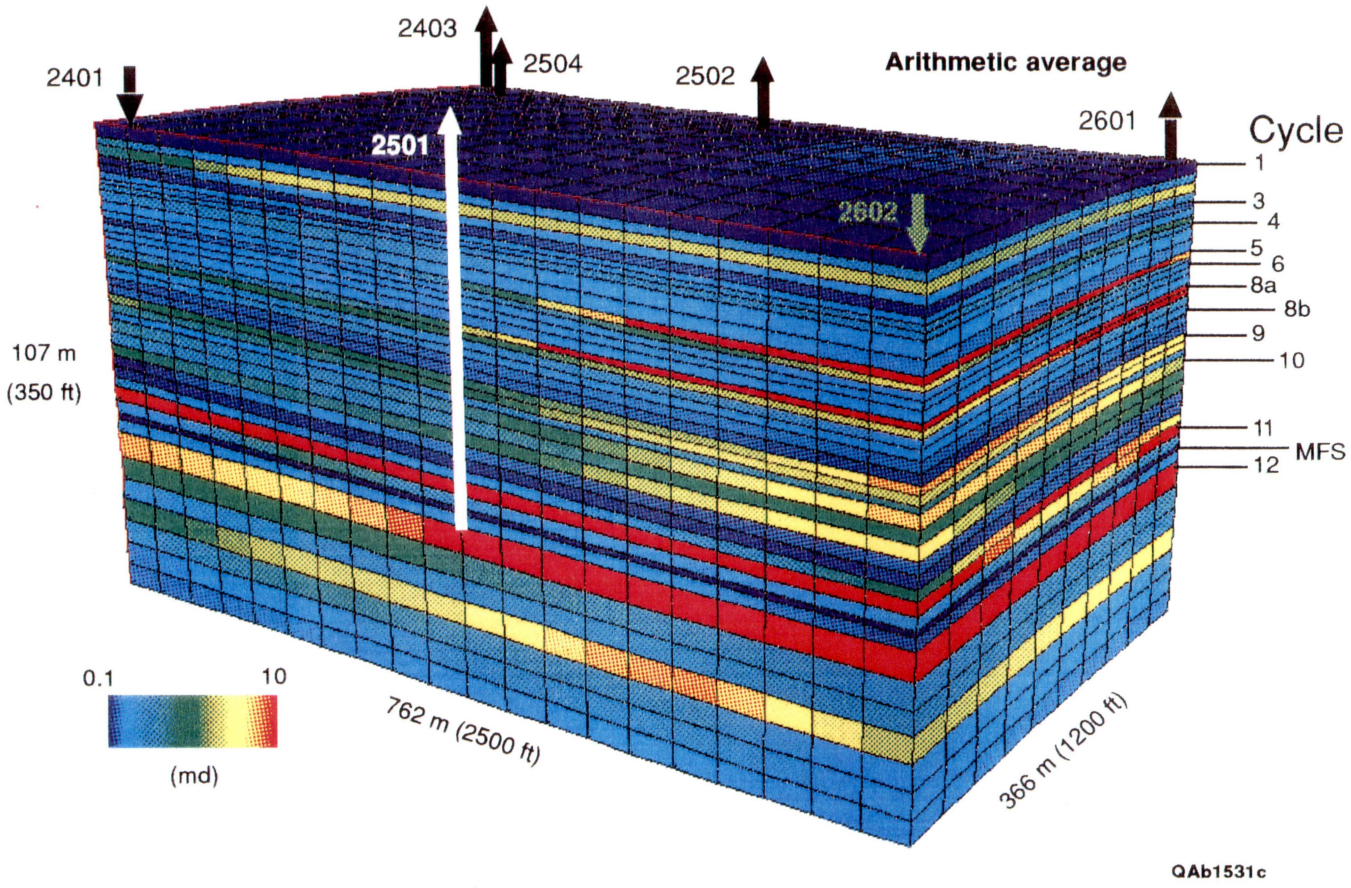

Figure 21. Permeability distribution in rock-fabric, 80-acre simulation model. The model contains 41 rock-fabric layers.

porosity. In addition, rock-fabric simulation models allow for easy inclusion of rock fabric-specific relative permeability curves in the model (Wang and others, 1994).

The 41-layer simulation model was used to simulate production from an 80-acre area within the two-section study area. The resulting image of the remaining oil saturation is more realistic than previous images, and recovery programs based on this type of image should provide more accurate performance predictions than previous images (Wang and others, 1994; Lucia and others, 1995).

Simulation studies have suggested that the predicted recoveries as estimated from rock-fabric-averaged models and geostatistical models constrained by a cycle framework are similar. However, the injection and production rates can be increased by using geostatistical models that have lateral spatial correlation of permeability within the rock-fabric facies (Grant and others, 1994). This indicates that the spatial distribution of permeability within rock-fabric facies may be important, but more studies are needed before its importance can be resolved.

The Seminole model, as well as other rock-fabric models of the Permian Basin now being studied, are based on approximately 1,000-ft- (330-m) spaced areal well data and 1-ft- (30-cm) spaced vertical core data. Because these models are developed in sufficient detail and closely resemble outcrop models, they can be used to construct and test geological and geostatistical methods for constructing reservoir images where well spacing is much greater that 1,000 ft.

REFERENCES

Galloway, W.E., Ewing, T.E., Garrett, C.E., Jr., Tyler, Noel, and Bebout, D.G., 1983, Atlas of major Texas oil reservoirs: The University of Texas at Austin, Bureau of Economic Geology, 139 p.

Grant, C.W., Goggin, D.J., and Harris, P.M., 1994, Outcrop analog for cyclic-shelf reservoirs, San Andres Formation of Permian Basin: Stratigraphic framework, permeability distribution, geostatistics, and fluid-flow modeling: American Association of Petroleum Geologists Bulletin, v. 78, no. 1, p. 23–54.

Kerans, Charles, Lucia, F.J., and Senger, R.K., 1994, Integrated characterization of carbonate ramp reservoirs using Permian San Andres Formation outcrop analogs: American Association of Petroleum Geologists Bulletin, v. 78, no. 2, p. 181–216.

Kerans, Charles, Lucia, R.J., Senger, R.K., Fogg, G.E., Nance, H.S., and Hovorka, S.D., 1993, Characterization of facies and permeability patterns in carbonate reservoirs based on

outcrop analogs: The University of Texas at Austin, Bureau of Economic Geology, final report prepared for the Assistant Secretary for Fossil Energy, U.S. Department of Energy, under contract no. DE-AC22-89BC14470, 160 p.

Kozeny, J.S., 1927 (no title available): Ber Wiener Akad. Abt. IIa, v. 136, p. 271.

Lucia, F.J., 1983, Petrophysical parameters estimated from visual descriptions of carbonate rocks: a field classification of carbonate pore space: Journal of Petroleum Technology, v. 35, no. 3, p. 629–637.

_____ 1995, Rock-fabric/petrophysical classification of carbonate pore space for reservoir characterization: American Association of Petroleum Geologists Bulletin, v. 79, no. 9, p. 1275–1300.

Lucia, F.J., and Conti, R.D., 1987, Rock fabric, permeability, and log relationships in an upward-shoaling, vuggy carbonate sequence: The University of Texas at Austin, Bureau of Economic Geology Geological Circular 87-5, 22 p.

Lucia, F.J., Kerans, Charles, and Wang, F.P., 1995, Fluid-flow characterization of dolomitized carbonate-ramp reservoirs: San Andres Formation (Permian) of Seminole field and Algerita Escarpment, Permian Basin, Texas and New Mexico, *in* Stoudt, E.L., and Harris, P.M., eds., Hydrocarbon reservoir characterization: geologic framework and flow unit modeling: SEPM (Society for Sedimentary Geology), SEPM Short Course No. 34, p. 129–153.

Lucia, F.J., Kerans, Charles, Senger, R.K., 1992, Defining flow units in dolomitized carbonate-ramp reservoirs: Society of Petroleum Engineers, Paper No. SPE 24702, p. 399–406.

Lucia, F.J., and Major, R.P., 1994, Porosity evolution through hypersaline reflux dolomitization, *in* Purser, B.H., Tucker, M.E., and Zenger, D.H., eds., Dolomites, a volume in honour of Dolomieu: International Association of Sedimentologists, Special Publication No. 21, p. 325–341.

Powers, R.W., 1962, Arabian Upper Jurassic carbonate reservoir rocks, *in* Ham, W.E., ed, Classification of carbonate rocks: a symposium: American Association of Petroleum Geologists Memoir No. 1, p. 122–192.

Senger, R.K., Lucia, R.J., Kerans, Charles, Ferris, M.A., and Fogg, G.E., 1993, Dominant control on reservoir-flow behavior in carbonate reservoirs as determined from outcrop studies, *in* Linville, Bill, ed., Burchfield, T.E., and Wesson, T.C., chairmen, eds., Reservoir characterization III: Proceedings, Third International Reservoir Characterization Technical Conference, Tulsa, Oklahoma, November 1991: Tulsa, PennWell Books, p. 107–150.

Swanson, B.J., 1981, A simple correlation between permeabilities and mercury capillary pressures: Journal of Petroleum Technology, vol. 33, p. 2498–2504.

Wang, F.P., Lucia, F.J., and Kerans, Charles, 1994, Critical scales, upscaling, and modeling of shallow-water carbonate reservoirs: Society of Petroleum Engineers, Paper No. SPE 27715, p. 765–773.

Wang, F.P., and Lucia, F.J., 1993, Comparison of empirical models for calculating the vuggy porosity and cementation exponent of carbonates from log responses: The University of Texas at Austin, Bureau of Economic Geology Geological Circular 93-4, 27 p.